Project Title: Spatial Epidemiology Modeling of the Florida Coral Disease Outbreak

Co-Principal Investigator:
Erinn Muller
Staff Scientist, Program Manager
Coral Health and Disease Program
Mote Marine Laboratory
emuller@mote.org

Co-Principal Investigator:
Robert van Woesik
Professor
Florida Institute of Technology
rvw@fit.edu

Student Contributor:
Constance Sartor
New College of Florida Graduate
Mote Marine Laboratory Intern
constance.sartor14@ncf.edu

Dates:
15 February 2018 – 30 June 2018

Background:
Coral diseases have caused widespread deterioration of coral reefs over the past five decades in both shallow and deep coral reef systems. However, very little is known about where, when, and why these coral disease outbreaks occur. Florida's coral reefs are currently experiencing a multi-year disease-related mortality event that has resulted in massive die-offs in multiple coral species. Approximately 21 species of coral, including both Endangered Species Act-listed and the primary reef-building species, have displayed tissue-loss lesions that often result in whole colony mortality. First observed near Virginia Key in late 2014, the disease has since spread to the northernmost extent of the Florida reef tract (FRT) and south into the lower Florida Keys. Understanding the etiology, or cause, of coral diseases requires a multi-faceted approach. In the absence of a definitive diagnosis, a characterized etiology, and an understanding of environmental drivers, it is difficult to implement management actions to potentially control the spread of the disease(s) and associated environmental co-factors, and/or treat or manage affected corals. The present project investigated the epizootiology (i.e., the disease ecology) of the Florida tissue-loss disease at multiple spatial and temporal scales.

Mapping the spatial distribution of disease prevalence within the FRT is critical to understanding the epizootiology of this outbreak (Muller and van Woesik, 2012, 2014; Randall *et al.*, 2014). The present disease outbreak already appears highly contagious among reefs, and anecdotal evidence suggests clustering within reef areas. Disease clusters are abnormally high numbers of individuals (or sites) within a defined area that exhibit similar disease signs. A clustered distribution of diseased sites, relative to the distribution of the entire coral population, suggests a contagious mode of disease transmission. Understanding the spatio-temporal dynamics of the disease outbreak will provide insight into the disease etiology and mode of disease transmission.

Following the movement of disease from one reef to another will determine whether the nearest reefs are more likely to get disease through time or if other environmental or ecological parameters influence the disease ecology. Alternatively, a spatially random distribution of disease infection may suggest that an entire region is infected simultaneously and diseased sites are more susceptible than non-diseased sites. Finally, the directional movement of newly infected sites will provide information on (i) how the disease is transmitted, (ii) whether particular species are more vulnerable than others, (iii) whether there is a distance threshold needed for transmission, and (iv) the rate at which this disease spreads within a region.

Staff from Florida Wildlife Research Institute's Center for Spatial Analysis (CSA) in St Petersburg, FL are currently addressing the need for a single, coordinated data management plan for the FRT. This effort includes creating a contact list for datasets currently used by federal, state, non-profit, and university researchers; acquiring the datasets and metadata; evaluating these for commonality, completeness, and consistency; and organizing these in a logical and comprehensive manner. The output of the CSA project was a geodatabase of datasets related to the current coral disease outbreak, which will assist researchers conducting additional analyses of the coral disease outbreak.

Goals and Objectives:

The present spatial epidemiology project modeled the disease progression using the multiple data sources compiled by CSA in the coral disease database. This dataset will help inform how the disease has progressed over the past four years, and may continue to spread across the FRT. The current analyses focus on large (10s of km) spatial dynamics to assess the broad-scale patterns of the disease ecology. The outcomes of this project will be incorporated into an on-going coral disease response effort, which seeks to improve understanding of the scale and severity of the Florida coral disease outbreak, identify primary and secondary causes, and identify potential management actions to remediate disease impacts, restore affected resources, and ultimately prevent future outbreaks.

Task Descriptions, Methodology, and Results:

***Data acquisition*:** All data used in the following tasks were curated by staff from CSA. A total of 26 different databases were provided by CSA staff to PIs Muller and van Woesik, which were contributed by at least a dozen different institutions. Data sets that were provided included those that documented coral diseases, coral community metrics, or water quality metrics (i.e., sea surface temperature, chlorophyll *a* concentrations, turbidity, nutrient concentrations, etc.). Each database provided these metrics collected at different temporal and spatial scales. PIs Muller and van Woesik selected key data sets into the following tasks and models to accomplish the project goals and objectives. In the future, additional data sets will be incorporated into the models to increase robustness.

Databases used: CREMP, SECREMP, FRRP DRM, IRMA, SEAFAN, and the Southern Disease Margin databases were used to create the spatial epidemiological maps (Task 1), which provided the disease front location for the northward and southward movement used in the spatial-temporal distance model (Task 1).[1] Additionally, these data were used to conduct the Ripley's K analysis to detect spatial clustering (Task 4). Only data that documented disease signs specific to the outbreak of tissue-loss disease in Florida were included in the analysis. These disease signs included those recorded as tissue loss or showing signs similar to white plague disease. In addition to these data sets, we also included the MODIS (NASA's Moderate Resolution Imaging Spectroradiometer) average monthly sea surface temperature layers and the average monthly chlorophyll *a* layers (a proxy for nutrients) into the data frame to explore potentially important covariates in the Bayesian general linear model analysis (Task 3). There are many additional data sets that can be included within the Bayesian model, however this project had a very short time window of only 4 months, from implementation to reporting.

Task 1: Create spatial epidemiological maps

Methods: Data were georeferenced and plotted onto basemaps within the ArcView GIS software package, which were used to create spatial epidemiological maps. Presence/absence of tissue-loss disease data were linked to the georeferenced dataset, which allowed the creation of a suite of spatial epidemiological maps that included kriging (i.e., a method of spatial interpolation) throughout the FRT. Kriging was used to predict the probability of disease within the spatial extent of the analysis, with a range from 0 (low probability) to 1 (high probability). Additionally, these maps provide a visual representation of disease hotspots through space and time. Initially, the spatial maps were created using quarterly, three-month time intervals, but the data were too sparse and the standard errors too high, showing low probability predictions. To overcome these

[1] Initialed data sources are the Coral Reef Ecosystem Monitoring Program (CREMP), Southeast Florida Coral Reef Evaluation and Monitoring Project (SECREMP), Florida Reef Resilience Program's Disturbance Response Monitoring (FRRP DRM), Post-Irma Ecosystem Assessment (IRMA), and Southeast Florida Action Network citizen science program (SEAFAN).

issues, data were considered annually, which resulted in low spatial standard error within the epidemiological maps.

Results: The 2014 annual map shows high variability among the disease information throughout the Florida Reef Tract (Figure 1). There appears to be a hotspot within the northern part of Broward County/southern Palm Beach County, which was driven primarily by four clustered disease sites. Two of these sites showed several colonies with tissue loss within species commonly documented with the current outbreak, *Dichocoenia stokesi*, *Meandrina meandrites*, and *Siderastrea siderea*. Whether this is the first indication of the disease outbreak or not is difficult to decipher at such a large spatial and temporal scale. Further survey or anecdotal information from this time period is essential for differentiating the location and timing of the disease onset. The 2014 data also indicates that there was some disease activity noted in the Florida Keys and in the Dry Tortugas, but these disease events were likely background levels of white plague disease and not related to the current epizootic event.

The 2015 annual map indicates a strong presence of the disease outbreak up into Broward County along the southeast coast of the Florida mainland (Figure 2). There was also a hotspot of activity offshore of Biscayne Bay in 2015, with higher disease levels reported within this area along the northern part of Biscayne Bay, offshore of Key Biscayne.

Along the northern boundary, a strong disease hotspot appears along the coast of Broward County in 2016, extending up to the northern parts of Palm Beach County (Figure 3). By 2016 there was a hotspot within the upper Florida Keys region, most likely related to the outbreak of tissue-loss disease. A disease hotspot appeared in the Dry Tortugas, but was likely not related to the present epizootic event.

In 2017, the disease front progressed south into the middle Florida Keys region, creating a relatively continuous hotspot of activity within that area (Figure 4). Reports collected near the end of 2017 indicate that the disease reached some of the western-most reef areas of the middle Florida Keys by the end of the year. Anecdotally, disease reached the northern-most section of the Florida Reef Tract during 2017, although there was limited data from that region.

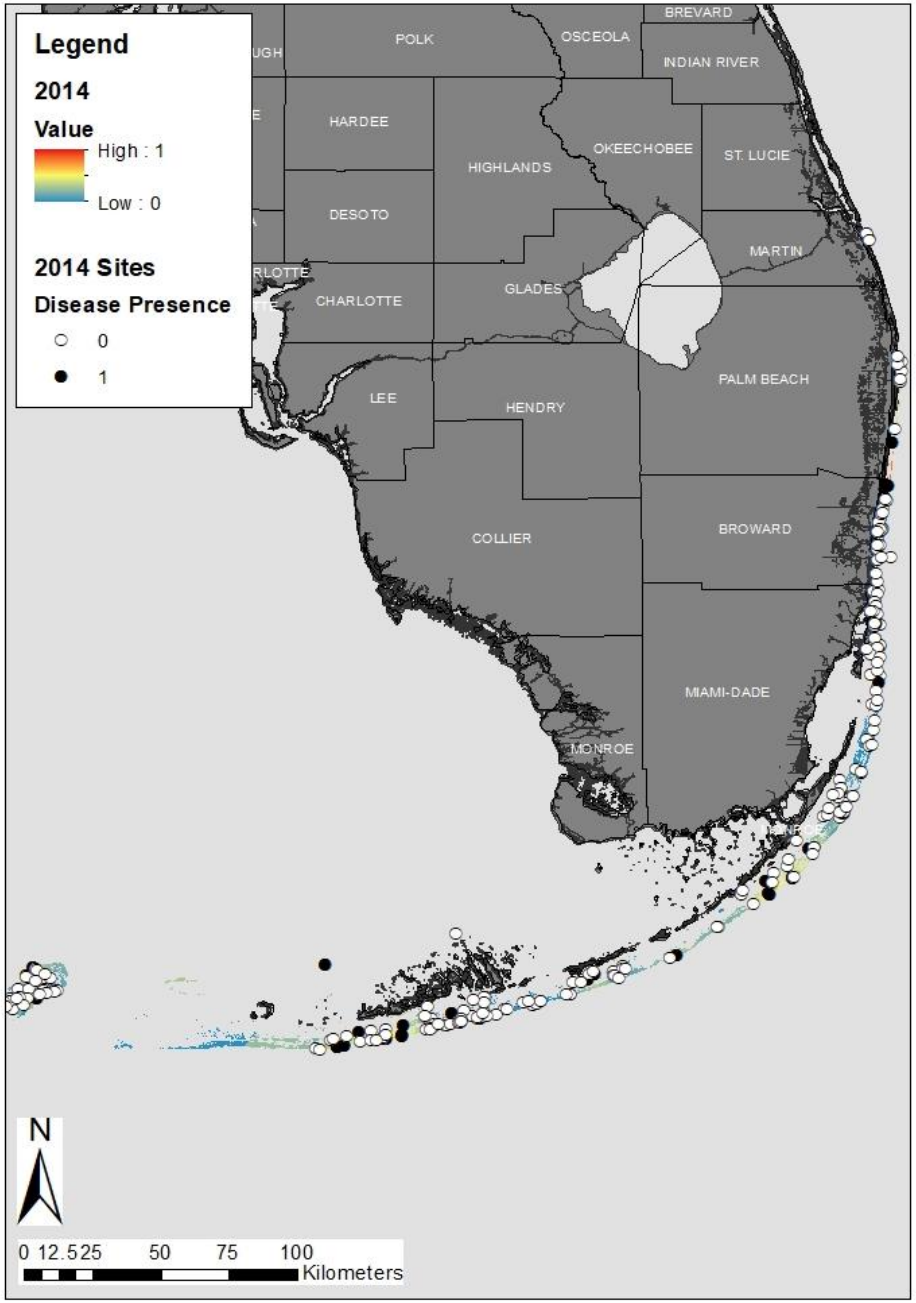
Legend
2014
Value
High : 1
Low : 0
2014 Sites
Disease Presence
0
1
BREVARD
POLK
OSCEOLA
INDIAN RIVER
HARDEE
HIGHLANDS
OKEECHOBEE
ST. LUCIE
DESOTO
MARTIN
CHARLOTTE
GLADES
LEE
HENDRY
PALM BEACH
COLLIER
BROWARD
MIAMI-DADE
MONROE
N
0 12.525 50 75 100
Kilometers

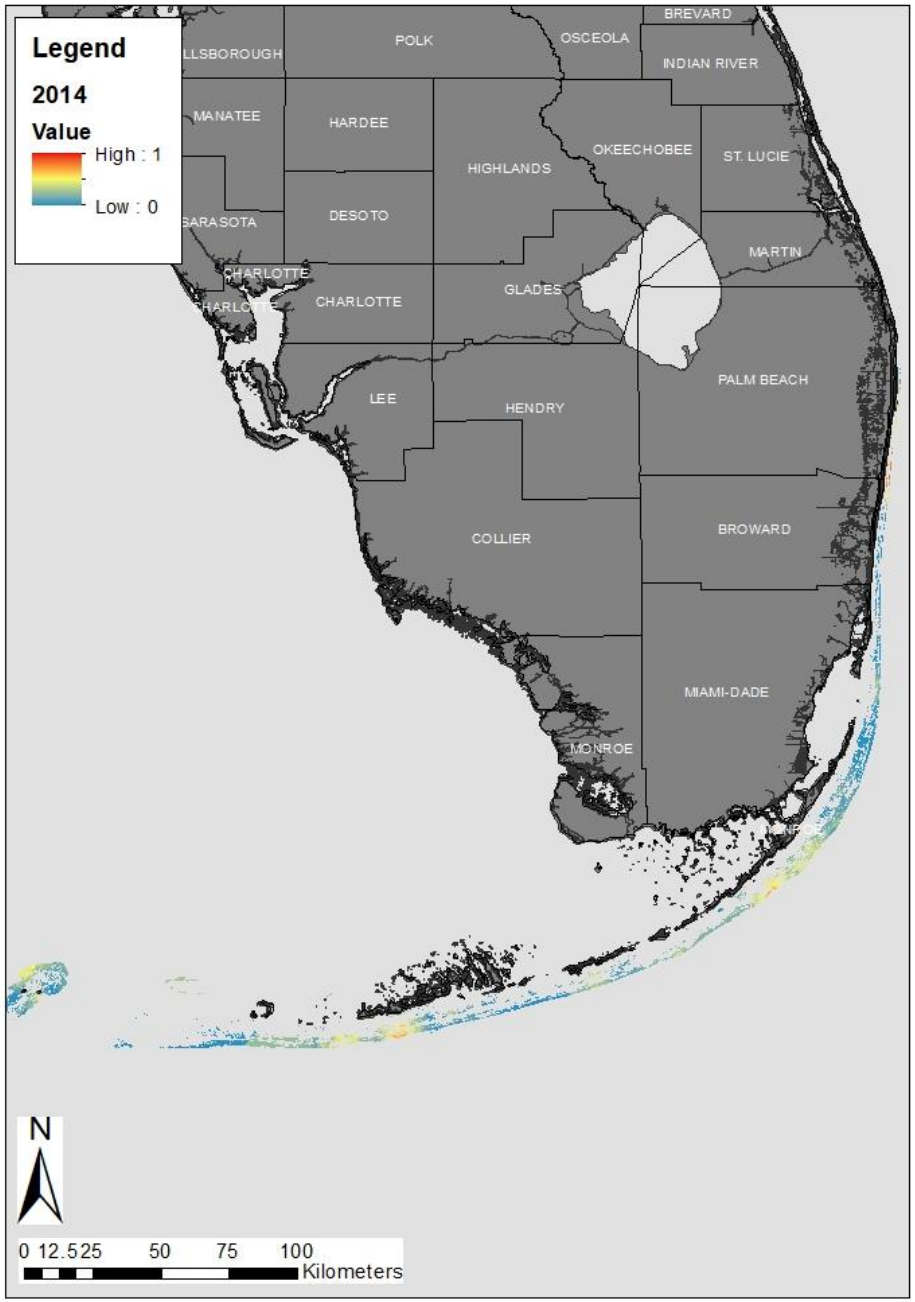
Legend
2014
Value
High : 1
Low : 0
BREVARD
POLK
OSCEOLA
INDIAN RIVER
MANATEE
HARDEE
HIGHLANDS
OKEECHOBEE
ST. LUCIE
SARASOTA
DESOTO
MARTIN
CHARLOTTE
GLADES
LEE
HENDRY
PALM BEACH
COLLIER
BROWARD
MIAMI-DADE
MONROE
N
0 12.525 50 75 100
Kilometers

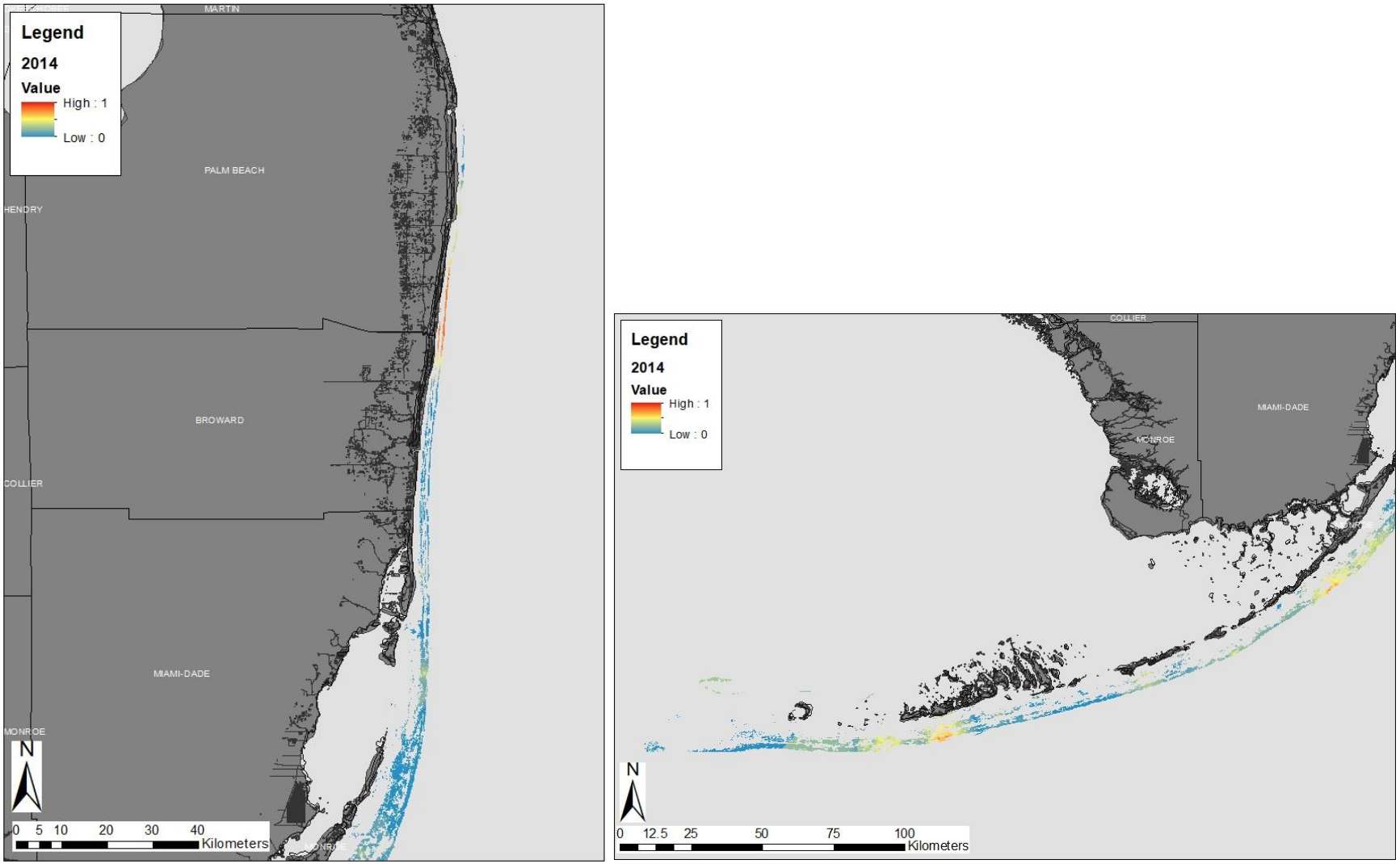

Figure 1. Epidemiological probability map of the tissue-loss disease outbreak during all of 2014. White dots indicate survey sites without disease present. Black dots represent survey sites with tissue loss disease present. Colors along the reef tract denote the probability of disease presence within the Florida Reef Tract. The disease probability map was created using Indicator Kriging in ArcGIS software. Warm colors represent high probability of the tissue loss-disease and cool colors represent low disease probability.

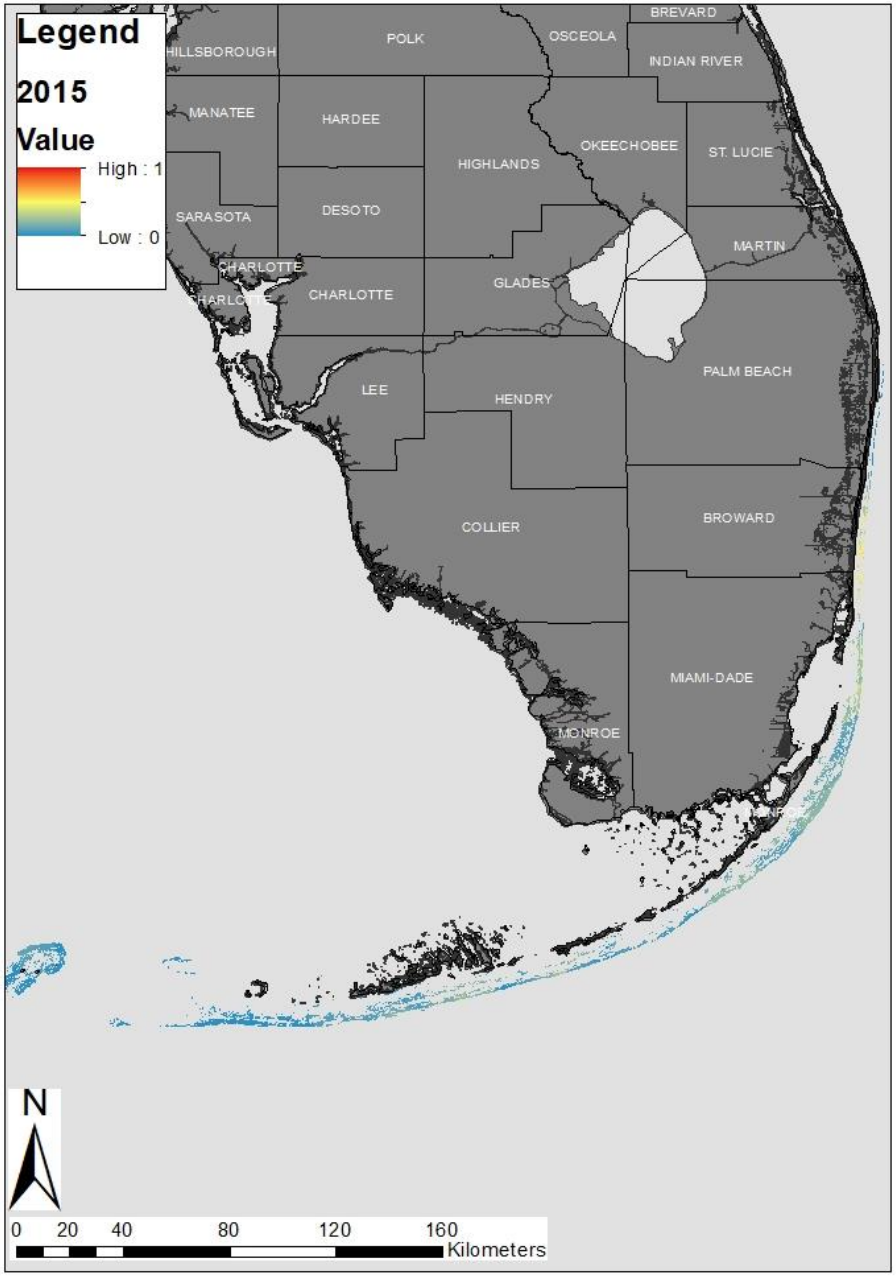
Legend
2015
Value
High : 1
Low : 0
HILLSBOROUGH
POLK
OSCEOLA
BREVARD
INDIAN RIVER
MANATEE
HARDEE
HIGHLANDS
OKEECHOBEE
ST. LUCIE
SARASOTA
DESOTO
MARTIN
CHARLOTTE
GLADES
LEE
HENDRY
PALM BEACH
COLLIER
BROWARD
MIAMI-DADE
MONROE
N
0 20 40 80 120 160
Kilometers

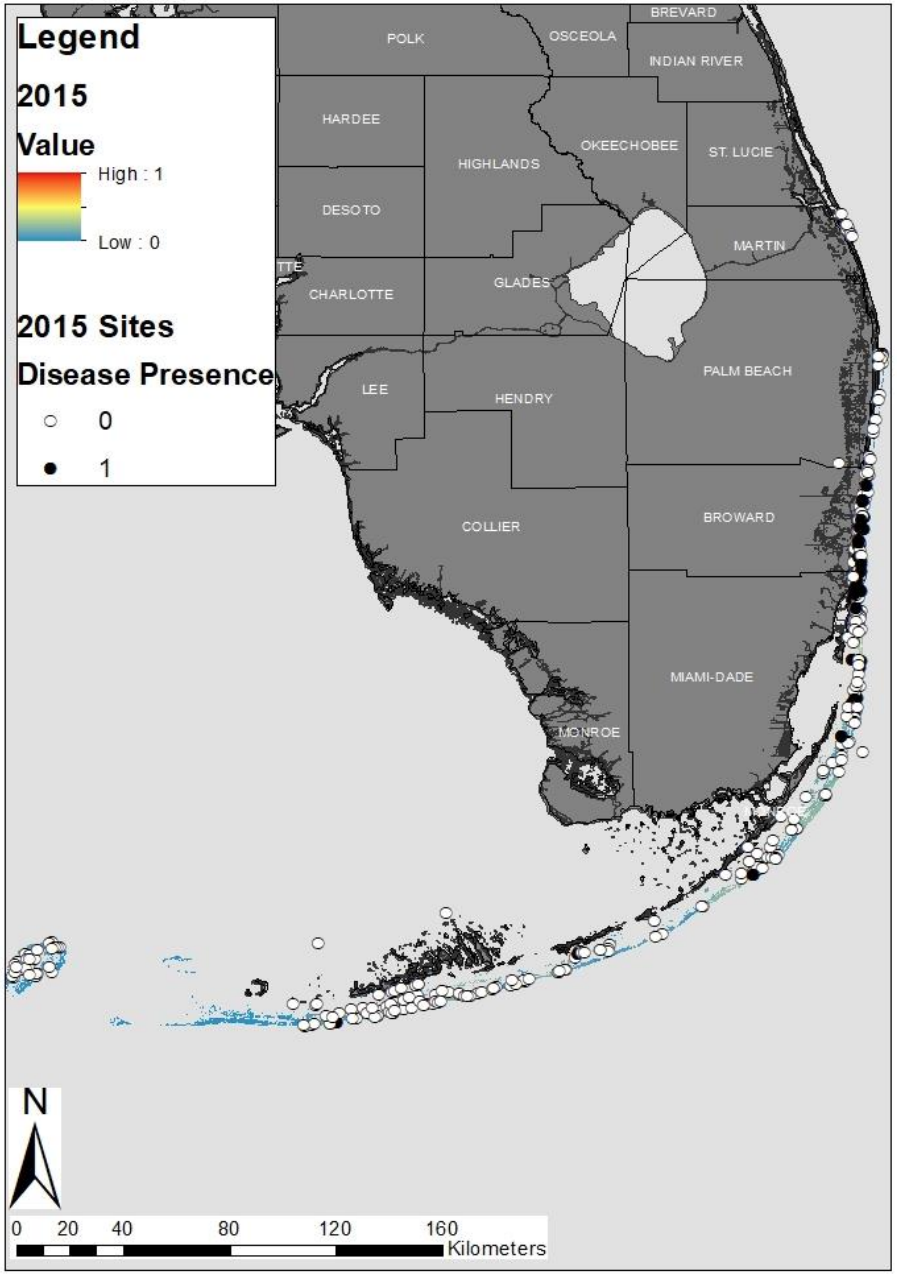
Legend
2015
Value
High : 1
Low : 0
2015 Sites
Disease Presence
0
1
POLK
OSCEOLA
BREVARD
INDIAN RIVER
HARDEE
HIGHLANDS
OKEECHOBEE
ST. LUCIE
DESOTO
MARTIN
CHARLOTTE
GLADES
LEE
HENDRY
PALM BEACH
COLLIER
BROWARD
MIAMI-DADE
MONROE
N
0 20 40 80 120 160
Kilometers

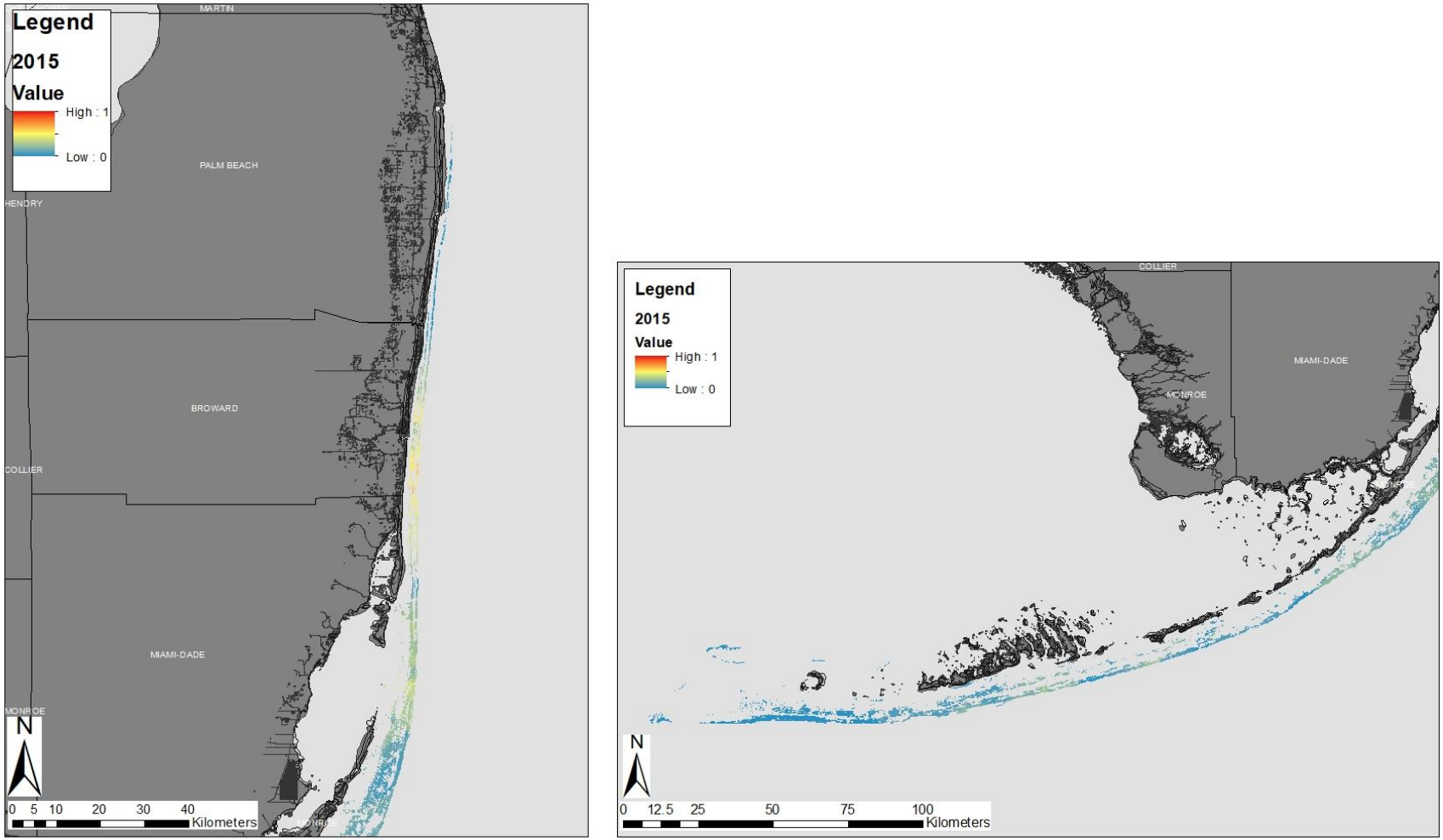

Figure 2. Epidemiological probability map of the tissue-loss disease outbreak during 2015. White dots indicate survey sites without disease present. Black dots represent survey sites with tissue loss disease present. Colors along the reef tract denote the probability of disease presence within the Florida Reef Tract. The disease probability map was created using Indicator Kriging in ArcGIS software. Warm colors represent high probability of the tissue-loss disease and cool colors represent low disease probability.

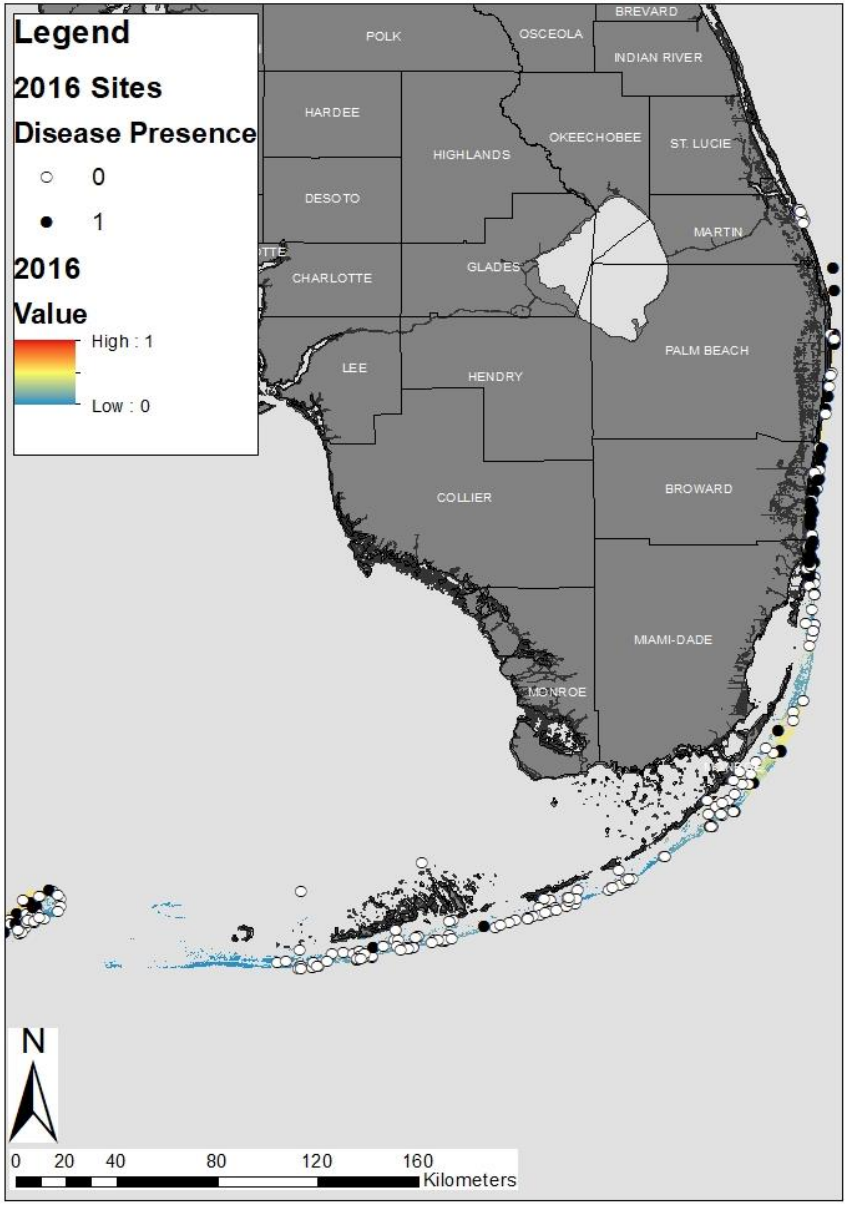
Legend
2016 Sites
Disease Presence
0
1
2016
Value
High : 1
Low : 0
POLK
OSCEOLA
BREVARD
INDIAN RIVER
HARDEE
HIGHLANDS
OKEECHOBEE
ST. LUCIE
DESOTO
MARTIN
CHARLOTTE
GLADES
LEE
HENDRY
PALM BEACH
COLLIER
BROWARD
MIAMI-DADE
MONROE
N
0 20 40 80 120 160
Kilometers

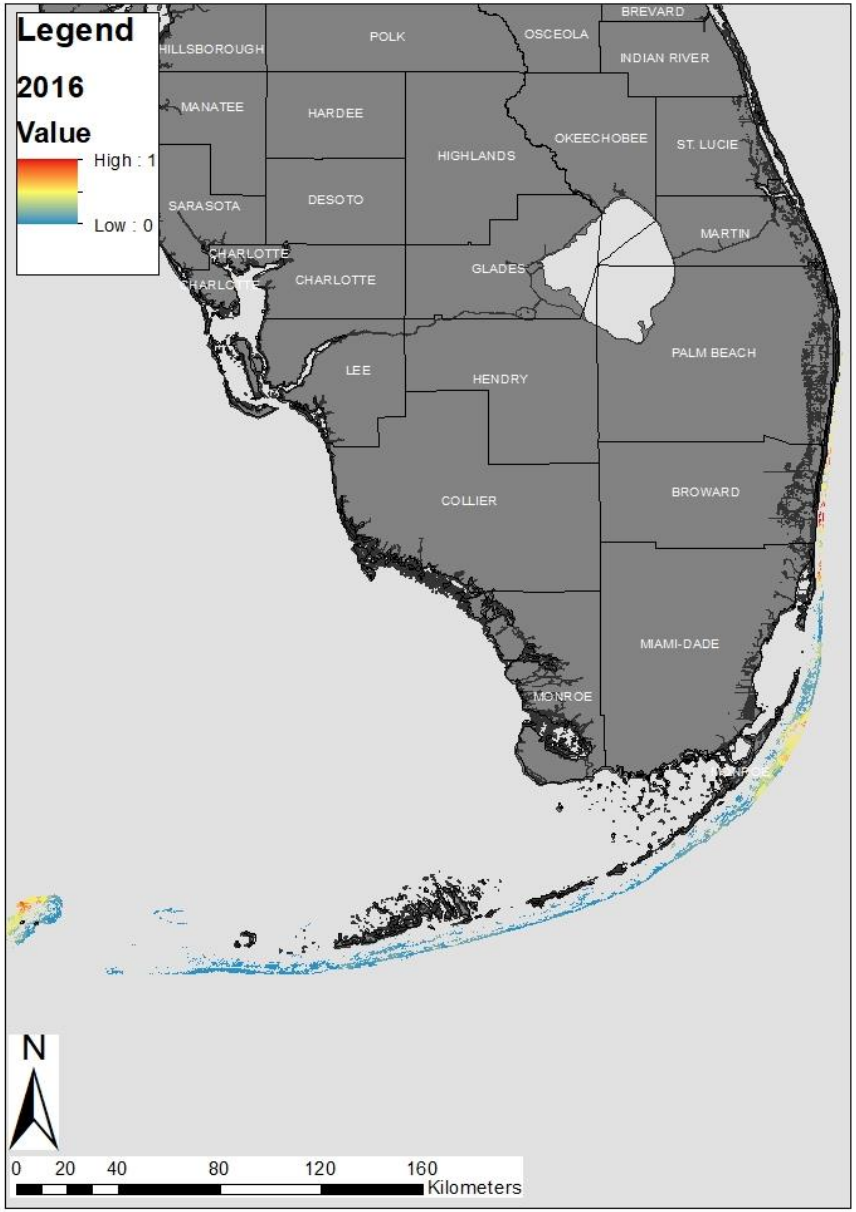
Legend
2016
Value
High : 1
Low : 0
HILLSBOROUGH
POLK
OSCEOLA
BREVARD
INDIAN RIVER
MANATEE
HARDEE
HIGHLANDS
OKEECHOBEE
ST. LUCIE
SARASOTA
DESOTO
MARTIN
CHARLOTTE
GLADES
LEE
HENDRY
PALM BEACH
COLLIER
BROWARD
MIAMI-DADE
MONROE
N
0 20 40 80 120 160
Kilometers

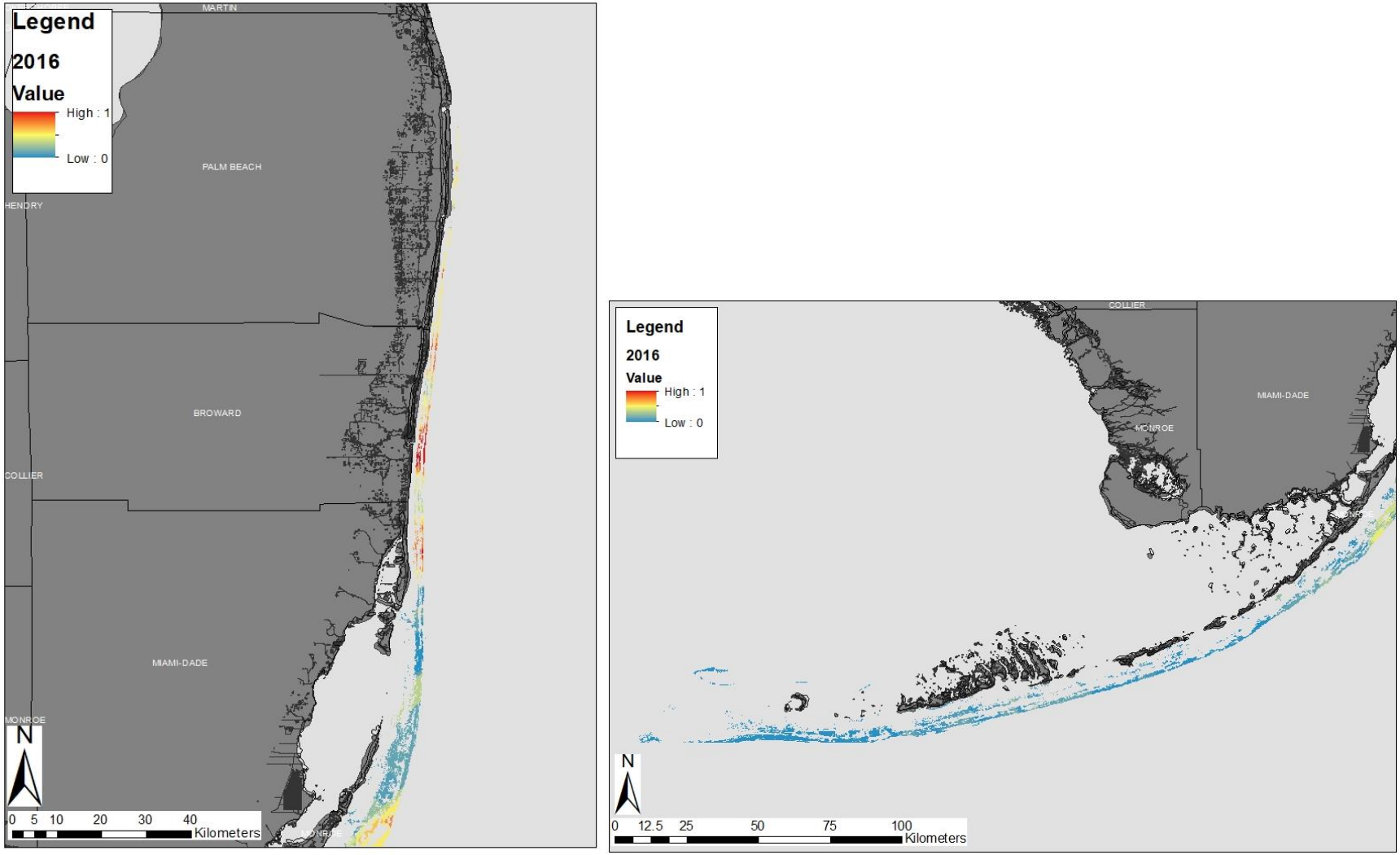

Figure 3. Epidemiological probability map of the tissue-loss disease outbreak during 2016. White dots indicate survey sites without disease present. Black dots represent survey sites with tissue loss disease present. Colors along the reef tract denote the probability of disease presence within the Florida Reef Tract. The disease probability map was created using Indicator Kriging in ArcGIS software. Warm colors represent high probability of the tissue-loss disease and cool colors represent low disease probability

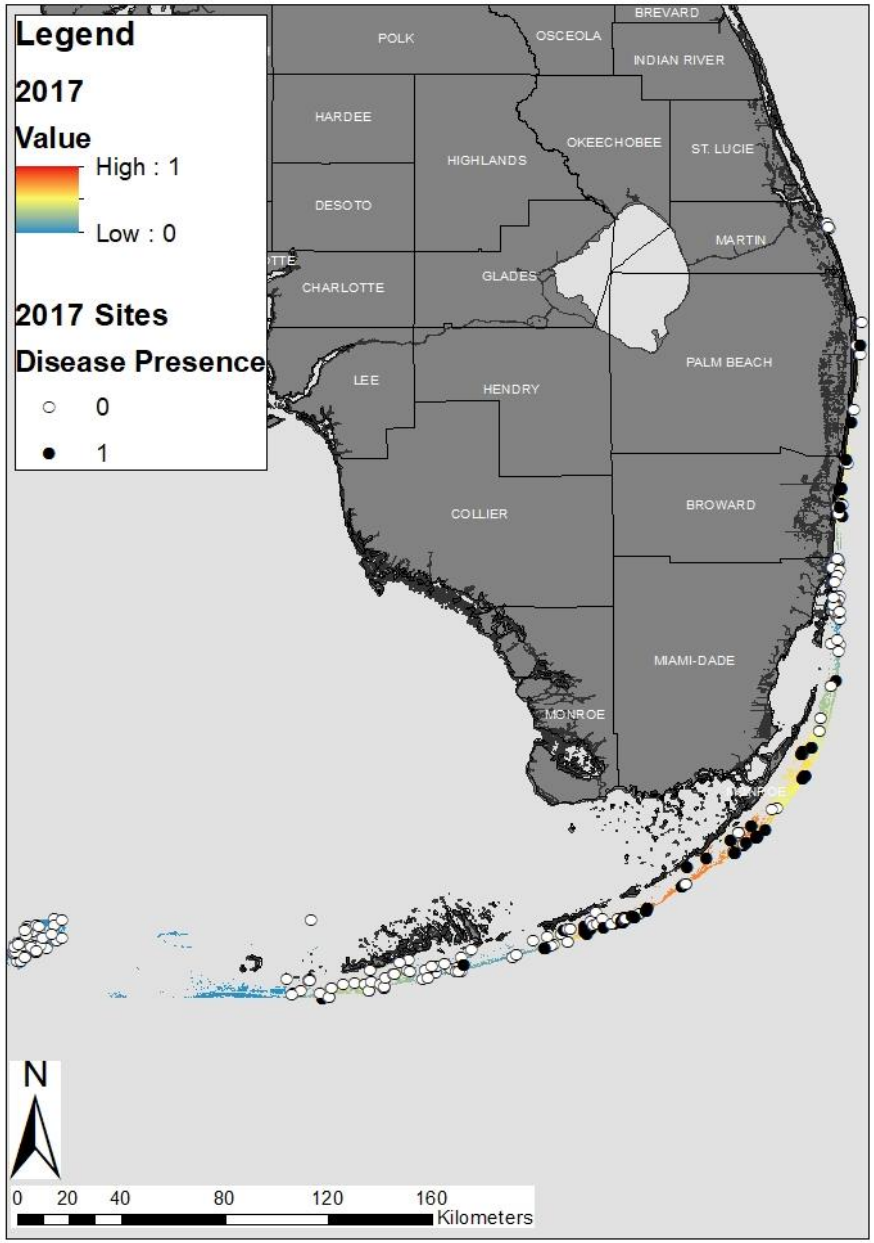
Legend
2017
Value
High : 1
Low : 0
2017 Sites
Disease Presence
0
1
POLK
OSCEOLA
BREVARD
INDIAN RIVER
HARDEE
HIGHLANDS
OKEECHOBEE
ST. LUCIE
DESOTO
MARTIN
CHARLOTTE
GLADES
LEE
HENDRY
PALM BEACH
COLLIER
BROWARD
MIAMI-DADE
MONROE
N
0 20 40 80 120 160
Kilometers

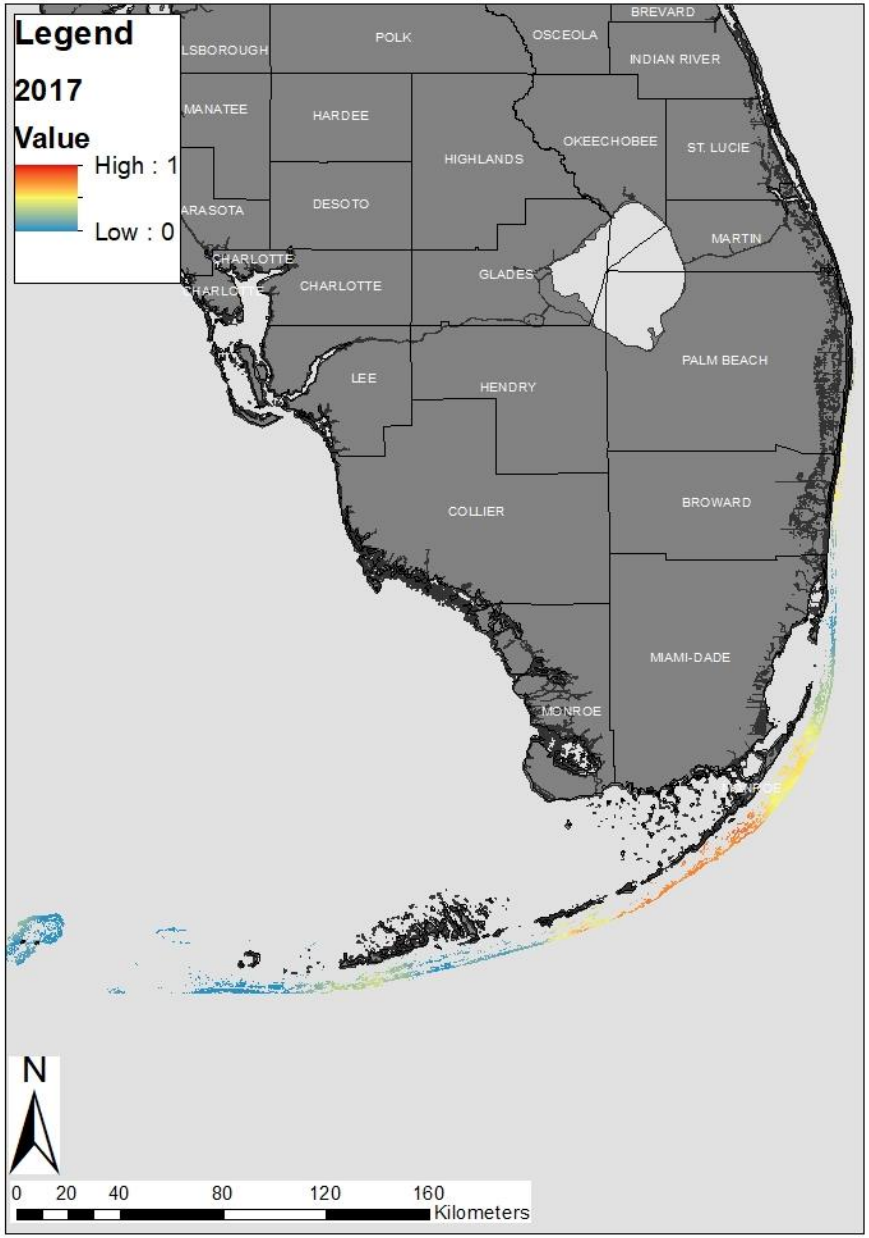
Legend
2017
Value
High : 1
Low : 0
POLK
OSCEOLA
BREVARD
INDIAN RIVER
MANATEE
HARDEE
HIGHLANDS
OKEECHOBEE
ST. LUCIE
DESOTO
MARTIN
CHARLOTTE
GLADES
LEE
HENDRY
PALM BEACH
COLLIER
BROWARD
MIAMI-DADE
MONROE
N
0 20 40 80 120 160
Kilometers

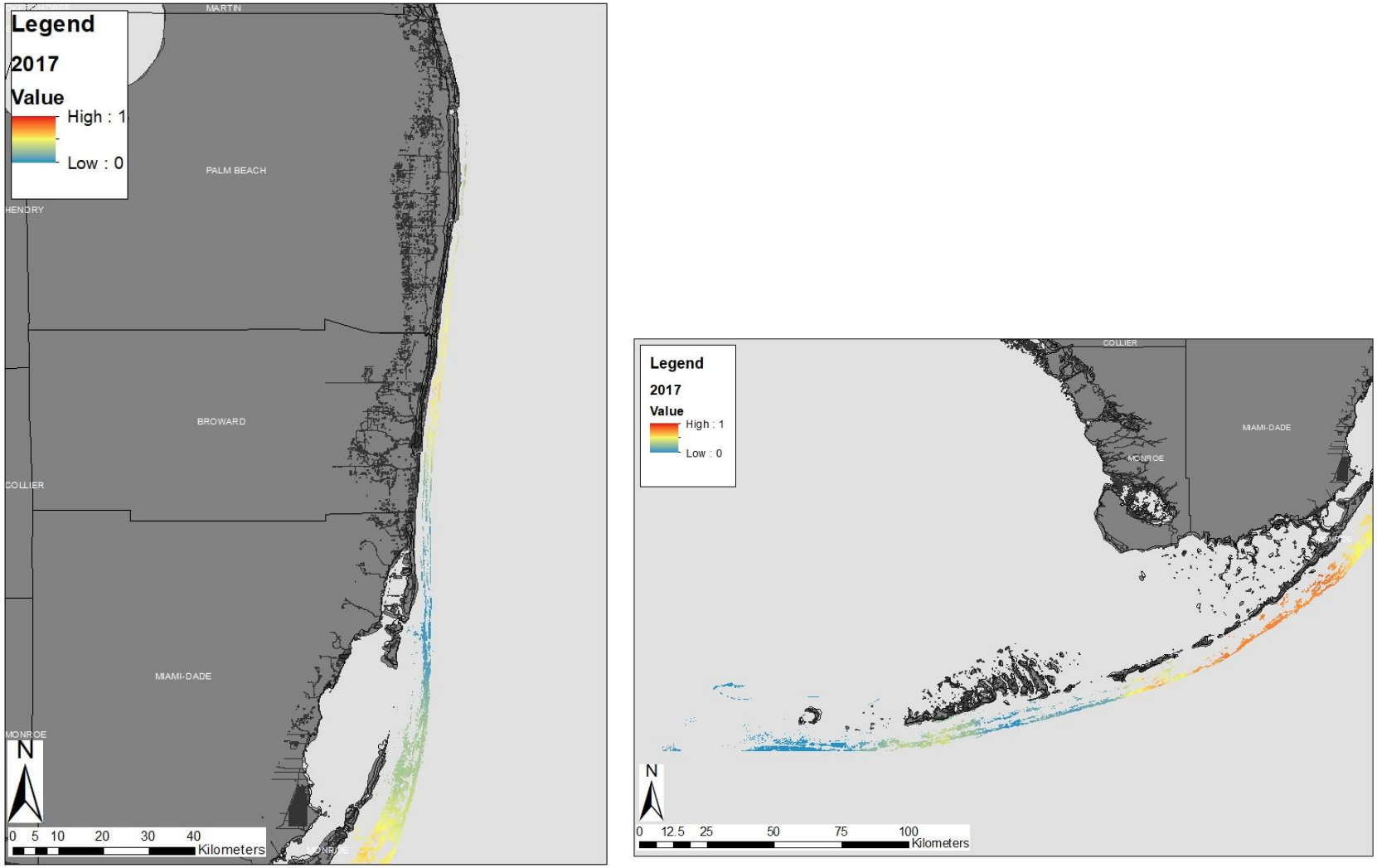

Figure 4. Epidemiological probability map of the tissue-loss disease outbreak during 2017. White dots indicate survey sites without disease present. Black dots represent survey sites with tissue loss disease present. Colors along the reef tract denote the probability of disease presence within the Florida Reef Tract. The disease probability map was created using Indicator Kriging in ArcGIS software. Warm colors represent high probability of the tissue-loss disease and cool colors represent low disease probability.

Task 2: Update contemporary spatio-temporal model

Methods: An initial mathematical model was created for the southeastern Florida disease outbreak information, which was created by PI van Woesik and presented in Precht et al., 2016. This model was updated with all the recent spatial information compiled in this report, spanning from Martin County into the middle Florida Keys, as the disease progressed from 2014 to 2017. All data were analyzed in the program R (R Core Team, 2017).

From all the combined data that were compiled, we first sought to find the leading edge of the disease along the FRT for every quarter from 2014 to 2018, and from there potentially identify and plot the coordinates of the leading edge of the disease (using 'sp' in R). We calculated the Euclidean distances between each quarterly-identified disease front (using the package 'geosphere' in R), and characterized the relationship between the time interval between recordings (as the predictor variable; x-axis) and the distance (m) the disease had potentially travelled (as the response variable; y-axis). The relationship appeared to follow an exponential function, therefore we used the package 'nls2' in R to find the coefficients (*a* and *z*) for the equation:

$$Distance \text{ the disease had travelled (m)} = a.\ Time^{z}$$

Results: We found a strong positive relationship between the time it took for the disease to spread south and the distance the disease had spread (Figure 5a). The speed at which the disease spread was somewhat slower that originally predicted by Precht et al. (2016). The difference between the two models was most likely a consequence of the more continuous nature of the reefs along which Precht *et al.* (2016) initially predicted the spread of the disease and the patchier nature of the reefs when the disease spread into the Florida Keys proper.

We took a similar approach to determine the spread of the disease to the north; however, the quarterly data was not rigorous. Therefore, we determined the spatial movement of the outbreak using annually amalgamated data. We again found a strong exponential relationship between time and distance (Figure 5b). Again, the most recently modeled disease estimates were considerably slower than the model originally proposed by Precht *et al.* (2016).

Interestingly, we found the same exponential equation was the best fit for both the northern and southern disease front data sets (Distance (m) = $1.857*\text{Time}^{1.571}$). These results suggest that the disease was moving at a similar rate both north and south from the point of origin; north, along the southeastern part of the mainland of Florida and south into the Florida Keys. These results could have important implications for interpreting the mode of disease transmission. For example, water flow rates may have less of an impact on transmission than was previously thought since the Florida Current would elicit a more direct and faster mode for transmission up the east coast of Florida compared with southern inshore eddy formations that move water south into and along the nearshore environment of the Florida Keys.

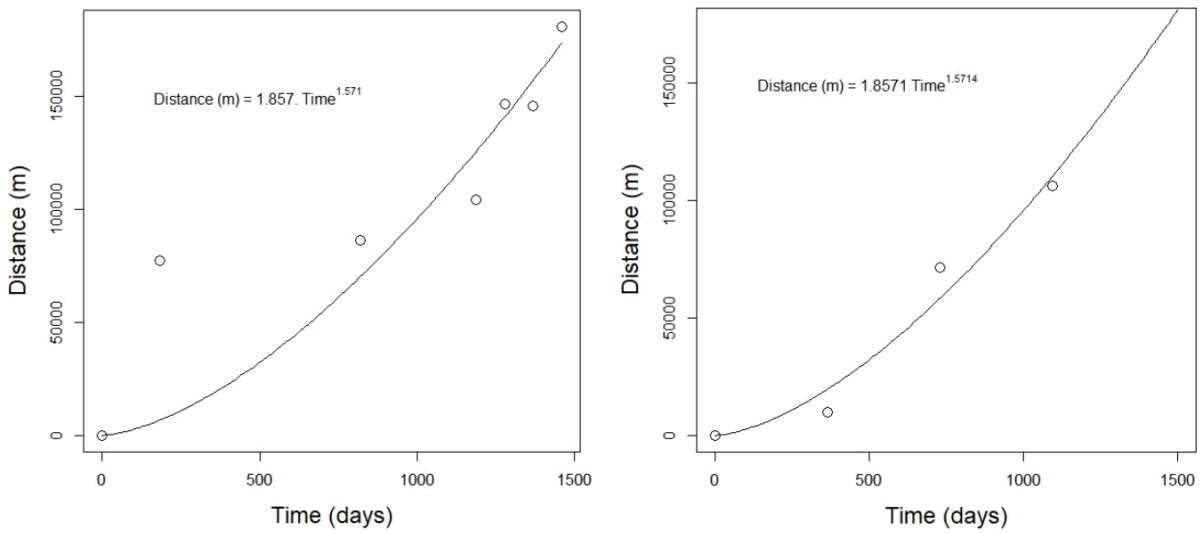

Figure 5. The relationship between the time it took the disease to spread, and the distance the disease had travelled to the a) **south** quarterly points and the b) **north** annual points of the initial outbreak.

Task 3: Conduct general linear models to determine potentially important co-variates that influence disease presence or absence and severity

Methods: A binomial general linear model analysis was conducted to determine the potential co-variates (coral density, coral diversity, water temperature, nutrients, etc) that may have influenced disease presence/absence within surveyed sites. All data were analyzed in the program R. The goal of this analysis was to determine whether there were particular environmental variables (e.g., water temperature, nutrients, depth) or ecological factors (e.g., presence of highly susceptible species) that influenced the likelihood of the tissue-loss disease occurring within a surveyed site. We ran an additional Poisson general linear model to determine whether these co-variates influenced the number of colonies with tissue-loss disease within each site. We included a total of 21 different ecological and environmental covariates including depth, coral density, coral species diversity, average monthly sea surface temperature, average monthly chlorophyll *a* concentrations, and the abundance of 16 different coral species. There are an additional ~20 water quality variables in addition to water current information and detailed coral cover information that are available within the data bases provided by CSA, of which several can be included within future analyses. However, integrating the vast sets of covariate data into comparable time and spatial scales of the disease database were not feasible within the current funding time frame.

Results: The most parsimonious binomial general linear model included the variables of coral density, coral diversity, average monthly sea surface temperature, average monthly chlorophyll *a* concentrations, and depth. The addition of the species level information reduced the quality of the model (i.e., increased the Akaiki's Information Criterion). Of the variables tested, three

showed a significant association with the presence or absence of disease within a site (Table 1). Sites with disease often had higher coral diversity, reduced sea surface temperature, and greater depth than sites without disease. Median coral diversity was 12 species in sites with disease and 10 species in sites without disease. Median sea surface temperature in sites with disease was 29.5 °C, whereas sites without disease had a median sea surface temperature of 29.7 °C. Sites with disease had a median depth of 9.3 meters, and sites without disease had a median depth of 7.1 meters.

Table 1. Results of the Binomial general linear model that tested the association of several ecological and environmental parameters on the presence/absence of disease within each site. Bolded parameters indicate a significant relationship.

Coefficients:

	Estimate	Standard Error	z value	p value
(Intercept)	-1.89405	2.01152	-0.942	0.346
Density	-0.13187	0.09085	-1.452	0.147
Diversity	**0.15027**	**0.06295**	**2.387**	**0.017**
SST	**-0.14977**	**0.06563**	**-2.282**	**0.023**
ChlA	0.26941	0.19126	1.409	0.159
Depth	**0.21237**	**0.04202**	**5.054**	**< 0.001**

The association between the tested covariates and the severity of disease in sites was determined using the Poisson general linear model, which used the number of diseased colonies as the predictor variable. There were six different variables that significantly influenced the number of corals with disease within sites: coral diversity, depth, average chlorophyll *a* concentrations, and the number of *Meandrina meandrites*, *Colpophyllia natans* and *Montastraea cavernosa* (Table 2). Coral diversity, depth, and chlorophyll *a* concentrations showed positive associations with the number of diseased colonies. Out of the three species of corals that significantly influenced the number of diseased corals, *M. meandrites* and *C. natans* showed negative associations with the predictor variable, indicating there were less numbers of these colonies within sites with disease. However, there was a positive association detected between *M. cavernosa* and the predictor variable indicating that the more colonies of this species within a site, the greater the number of diseased colonies recorded.

Table 2. Results of the Poisson general linear model that tested the association of several ecological and environmental parameters on the number of diseased corals within each surveyed site. Bolded parameters indicate a significant relationship.

Coefficients:

	Estimate	Standard Error	z value	p value
(Intercept)	**-5.68508**	**1.73133**	**-3.284**	**0.001**
Density	-0.05672	0.05683	-0.998	0.318
Diversity	**0.16648**	**0.04684**	**3.554**	**< 0.001**
Depth	**0.34188**	**0.0384**	**8.903**	**< 0.001**
SST	-0.08496	0.05688	-1.494	0.135
ChlA	**0.42851**	**0.13205**	**3.245**	**0.001**
MME	**-0.49149**	**0.1196**	**-4.11**	**< 0.001**
DSTO	0.07942	0.08758	0.907	0.364
CNAT	**-0.38805**	**0.11453**	**-3.388**	**< 0.001**
DLAB	0.10556	0.27395	0.385	0.701
MCAV	**0.09627**	**0.02361**	**4.078**	**< 0.001**

Task 4: Determine whether the disease follows contagion model

Methods: We tested whether the disease outbreak followed a predictable contagion spatial model, which would indicate that the outbreak was and potentially still is indeed contagious. Modified Ripley's K analyses for spatial clustering were applied to the disease presence/absence data, similar to Muller & van Woesik (2012). These analyses tested for significant spatial clustering, but also determined the radius of the clusters (i.e., the distance that corals are at risk for contagious disease transmission). All data were analyzed in the program R.

Using Ripley's K analysis as a spatial point pattern process (Haase, 1995), disease clustering was assessed each year for the entire FRT. Spatial distributions of sites with disease were analyzed using the adjusted Ripley's function, K(r), defined as the expected number of sites within a distance (r) from an arbitrary site. The function was normalized by dividing by the mean number of sites per unit area. Therefore, Ripley's K was calculated as:

$$\hat{K}(r) = \frac{A}{n^2} \sum_{i=1}^{n} \sum_{j=1, j \neq 1}^{n} \frac{I_r(d_{ij})}{w_{ij}},$$

where A was the total area of the region, n was the number of diseased sites, and d_{ij} was the distance between any two diseased sites i and j. $I_r(d_{ij})$ indicates whether or not there was a diseased site within distance r from site i. Therefore, $I_r(d_{ij})$ had a value of 1 if $d_{ij}<r$ and 0 otherwise. Because the study area was finite, w_{ij} represents the portion of the circumference of each circle that falls outside of the previously defined location area (Gatrell *et al.*, 1996).

Ripley's K identified disease clusters by comparing the spatial distribution of diseased sites with the distribution of all surveyed sites. The Ripley's K statistic was used to quantify non-random

clustering patterns of diseased sites within an area in terms of the degree and spatial scale of aggregation. The Ripley's K statistic, however, was standardized to account for the spatial aggregation of susceptible individuals within the study area (see Zvuloni *et al.*, 2009). A randomization technique was used to determine whether the *n* diseased sites found within the sampled area were significantly spatially aggregated, as compared with the aggregation found in the population of all surveyed sites using a null hypothesis approach. The transformation, referred to as Besag's *L* function, was calculated as:

$$L(r)=\sqrt{\frac{K(r)}{\pi}}-r$$

With this scaling, sites that had a Poisson spatial distribution resulted in the expected value of $L(r)=0$. A null distribution for L(r) was generated from a group of n sites and repeated 1,000 times so that L(r) was calculated for each group of n sites for any value of r. These results created a 95% confidence interval envelope for *L(r)*. *L(r)* was then calculated using only diseased sites to produce a new value, *LD(r),* and compared with the *L(r)* null envelope. Any value that resided outside of the envelope indicated either spatial clumping (above the *LD(r)*) or over-dispersion (below the *LD(r)*) of diseased sites.

Results: Each annual analysis showed significant clustering of diseased sites, although the radius of the cluster varied considerably through time (Figure 6). Results from the 2014 data show a small cluster window with a radius of ~21,000 m (21 km) (Figure 6a). These results suggest an approximate 42 km wide cluster of disease activity. In 2015 and 2016, however, significant clustering was detected throughout the majority of the spatial range of these two years of analyses. The Besag's L value exceeded the null distribution at a radius of approximately 1,000 m (1 km) in distance. The L values continued to be significant at a radius above this value for the rest of the spatial scales explored, although peak clustering occurred at ~30,000 m (30 km) in 2015 and ~40,000 m (40 km) in 2016 (Figures 6b, 6c). Within the 2017 and 2018 analyses the disease clustering again was more focused and less widespread. In 2017 the significant cluster radius ranged from ~1,000 to 20,000 m (1 – 20 km) and ~ 10,000 to 40,000 m (10 – 40 km) in 2018 (Figures 6d, 6e). These results reflect the widespread nature of the disease outbreak during the 2015 and 2016 time frame, and the more focused disease cluster within the 2017 and 2018 time frame, potentially a result of the disease having already passed through the northern reef limits and the Upper Keys, and presently impacting mainly the middle Florida Keys region.

These results also lead us to suggest an additional and testable hypothesis: that having a gap in the reef scape exceeding 80 km, the total diameter of the major clustering observed over the last four years, may reduce the likelihood of spread in the disease outbreak. Whether or not the outbreak infects the Bahamas or Cuba, the two closest reef scapes farther than 80 km in distance, may be the first test of this hypothesis. Special attention should be placed on surveying the Bimini islands of the Bahamas for tissue loss, which is approximately 80 km east of Miami.

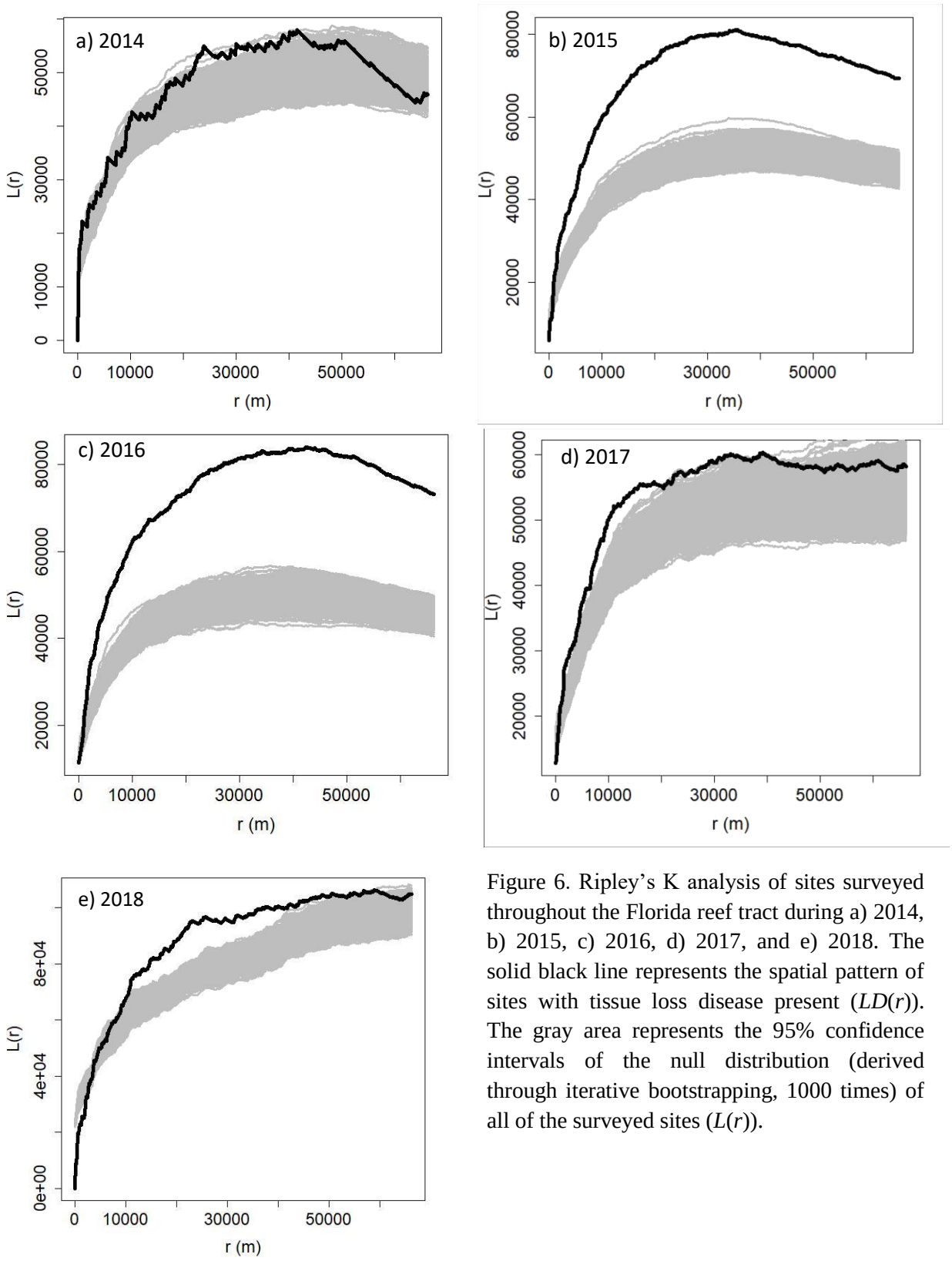

Figure 6. Ripley's K analysis of sites surveyed throughout the Florida reef tract during a) 2014, b) 2015, c) 2016, d) 2017, and e) 2018. The solid black line represents the spatial pattern of sites with tissue loss disease present ($LD(r)$). The gray area represents the 95% confidence intervals of the null distribution (derived through iterative bootstrapping, 1000 times) of all of the surveyed sites ($L(r)$).

Conclusions

The results of these modeling efforts support the conclusion that the outbreak is following spatial and temporal patterns consistent with a contagious disease. The interpolation maps show the disease outbreak became apparent in 2015, with an origination point somewhere along the southeast coast of Florida, within Broward County. The disease appeared to spread north and south over the next several years. Additionally, the Ripley's K analysis suggested significant spatial clustering each year, with varying size clusters through time. The disease was difficult to differentiate in 2014 with slight clustering at 21 km, became more prevalent and widespread in 2015 and 2016, and then again became more concentrated in 2017 and 2018. By this time the disease had already impacted the northern extent of the FRT, and was mainly affecting reefs within the middle Florida Keys. The Ripley's K analysis also showed peak clustering at a 40-km radius, suggesting that the disease may be limited to an 80-km diameter of reef; follow up studies will determine whether this is a regional artifact. Interestingly, the disease spread was slower than previously predicted and appeared to follow the same spatio-temporal exponential function moving both north along the southeast coast of Florida and south into the Florida Keys. These results suggest that water velocity and flow may have less of an effect than previously thought, although waterborne transmission is still likely. Follow up studies exploring small spatial scales with high-frequency disease data information, which can also be combined with water flow rates will help tease apart the broad-scale conclusions from the present analysis.

The general linear models, which tested the influence of 21 different covariates, showed that coral species diversity and depth were positively associated with disease presence, suggesting that deeper sites and sites with more coral diversity were at a greater risk of having disease. Sea surface temperature showed a negative association with disease presence, although the effect size of this variable was small, perhaps indicating the difference is ecologically irrelevant. Finally, severity of disease within sites was positively associated with coral diversity, depth, Chlorophyll *a* concentrations, and the number of *M. cavernosa* within the site. Further models should explore the additional water quality parameters to determine whether nutrients measured directly also show the same association as Chlorophyll *a* concentrations. The negative associate of *M. meandrites* and *C. natans* with disease severity may suggest that these corals were highly susceptible to the disease and losses of these species prior to the survey may have occurred.

Literature Cited

Gatrell AC, Bailey TC, Diggle PJ, Rowlingson BS, Rowlingsont BS. (1996). Point Spatial application pattern analysis geographical epidemiology. *Trans Inst Br Geogr* **21**: 256–274.

Haase P. (1995). Spatial pattern analysis in ecology based on Ripley's K-function: Introduction and methods of edge correction. *J Veg Sci* **6**: 575–582.

Muller EM, Van Woesik R. (2012). Caribbean coral diseases: Primary transmission or secondary infection? *Glob Chang Biol* **18**: 3529–3535.

Muller EM, Van Woesik R. (2014). Genetic susceptibility, Colony size, and water temperature drive white-pox disease on the coral *Acropora palmata*. *PLoS One* **9**. e-pub ahead of print, doi: 10.1371/journal.pone.0110759.

Precht WF, Gintert BE, Robbart ML, Fura R, van Woesik R. (2016). Unprecedented Disease-Related Coral Mortality in Southeastern Florida. *Sci Rep* **6**: 31374.

R Core Team. (2017). R Core Team (2017). R: A language and environment for statistical computing. *R Found Stat Comput Vienna, Austria URL http//wwwR-project.org/* R Foundation for Statistical Computing.

Randall CJ, Jordan-Garza AG, Muller EM, Van Woesik R. (2014). Relationships between the history of thermal stress and the relative risk of diseases of Caribbean corals. *Ecology* **95**: 1981–1994.

Zvuloni A, Artzy-Randrup Y, Stone L, Kramarsky-Winter E, Barkan R, Loya Y. (2009). Spatio-temporal transmission patterns of black-band disease in a coral community. *PLoS One* **4**. e-pub ahead of print, doi: 10.1371/journal.pone.0004993.

Funding

Funding for this project was provided by the State of Florida, as administered by the Florida Department of Environmental Protection, Florida Coastal Office, Southeast Region. Purchase Order No. B29704.